Simulated Moving Bed Multiobjective Optimization Using Standing Wave Design and Genetic Algorithm

Ki Bong Lee and Rahul B. Kasat
School of Chemical Engineering, Purdue University, West Lafayette, IN 47907

Geoffrey B. Cox
Chiral Technologies, West Chester, PA 19380

Nien-Hwa Linda Wang
School of Chemical Engineering, Purdue University, West Lafayette, IN 47907

DOI 10.1002/aic.11604
Published online October 13, 2008 in Wiley InterScience (www.interscience.wiley.com).

Multiobjective optimization of simulated moving bed systems for chiral separations is studied by incorporating standing wave design into the nondominated sorting genetic algorithm with jumping genes. It allows simultaneous optimization of seven system and five operating parameters to show the trade-off between productivity, desorbent requirement (DR), and yield. If pressure limit, product purity, and yield are fixed, higher productivity can be obtained at a cost of higher DR. If yield is not fixed, it can be sacrificed to achieve higher productivity or vice versa. Short zones and high feed concentration favor high productivity, whereas long zones favor high yield and low DR. At fixed product purity and yield, increasing the pressure limit allows the use of smaller particles to increase productivity and to decrease DR. The performance of low-pressure simulated moving bed can be improved significantly by using shorter columns and smaller particles than those in conventional systems. © 2008 American Institute of Chemical Engineers *AIChE J,* 54: 2852–2871, 2008
Keywords: simulated moving bed chromatography, multiobjective optimization, standing wave design, genetic algorithm, chiral separation, NSGA-II-JG

Introduction

Simulated moving bed (SMB) chromatography is a major separation technology and has been used in petrochemical and sugar industries for decades.[1–5] Recently, SMB has been used for the purification of fine chemicals and pharmaceuticals, particularly for the production of single enantiomers.[6–8]

In an SMB process, a continuous counter-current flow between the mobile phase and the stationary phase is mimicked by advancing the inlet (feed and desorbent) and the outlet (extract and raffinate) ports periodically by one column length in the direction of the mobile phase flow (Figure 1). In this operation, the fast-migrating solute is recovered from the raffinate port whereas the slow-migrating solute is recovered from the extract port. Since the products are drawn from the nonoverlapping regions, high product purity and high yield can be achieved. Overlapping of the two migrating

Correspondence concerning this article should be addressed to N.-H. L. Wang at wangn@ecn.purdue.edu.
Current addresses: K. B. Lee, Alternative Fuels Research Center, Korea Institute of Energy Research, Daejeon 305-343, Korea; R. B. Kasat, Central Research and Development, E. I. du Pont de Nemours and Company, Inc., Experimental Station, Wilmington, DE 19880.

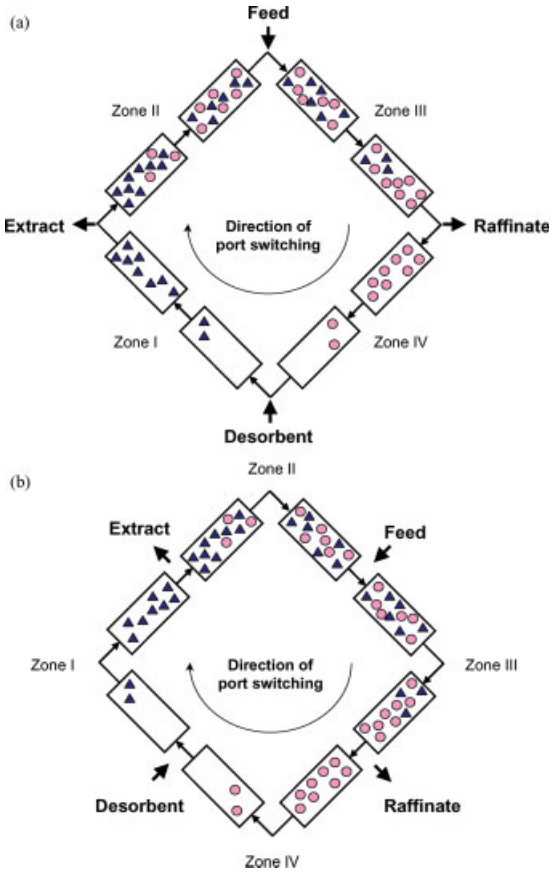

Figure 1. Schematic of a conventional four-zone simulated moving bed. (a) step N and (b) step N + 1.

[Color figure can be viewed in the online issue, which is available at www.interscience.wiley.com.]

bands in SMB, results in high adsorbent utilization, high product concentration, and low solvent consumption. In general, SMB requires less adsorbent and desorbent in a specific separation than conventional batch chromatography.[4]

Design and construction of SMB systems usually aim to maximize production capacities and to minimize separation cost, while satisfying constraints such as product purity and maximum system pressure. The factors which affect the economics of a given separation process are usually multiple and are often in conflict with each other. Therefore, it is important to formulate SMB optimization problems as multiobjective optimization problems. Decision variables for SMB optimization generally include seven system parameters (particle size, column length, the number of columns in each zone, and feed concentration), and five operating parameters (four zone velocities and switching time).

There have been several studies on the multiobjective optimization of SMB systems. Most of these studies used Genetic Algorithm (GA) as an optimization tool. GA originated from the studies of Holland.[9] GA mimics the process of natural selection and natural genetics. Several studies extended GA to solve more realistic multiobjective optimization problems.[10] Among them, Srinivas and Deb[11] developed the nondominated sorting genetic algorithm (NSGA). In 2002, Deb et al.[12] modified NSGA by incorporating the concept of elitism and developed more efficient NSGA-II (elitist NSGA). Elitism preserves the best solutions obtained over various generations. This strategy rapidly increases the performance of GA, since it prevents the loss of the already found best solutions in the selection process. Kasat and Gupta[13] recently incorporated the concept of jumping genes (JGs), which is borrowed from biology, to NSGA-II, resulting in NSGA-II-JG algorithm (elitist NSGA with JGs). The JG operator improved the diversity of the mating pool resulting in much better spreading of solutions and increasing the convergence speed. Kasat and Gupta[13] successfully applied NSGA-II-JG algorithm to the multiobjective optimization of an industrial fluidized-bed catalytic cracker unit.

Table 1 summarizes the key features of the previous GA-based multiobjective optimization studies for SMB systems. Zhang et al.[14] first applied NSGA to the multiobjective optimization of SMB. They compared SMB and Varicol processes which were optimized either for maximum purity in both extract and raffinate products or for maximum throughput with minimal desorbent consumption. Subramani et al.[15] optimized SMB system for isolation of fructose from a mixture of glucose and fructose solution. Either the simultaneous optimization of productivity (PR) and purity of the fructose product or simultaneous optimization of both PR of both products were performed. Zhang et al.[16] studied the effects of particle size, total number of columns, and feed concentration on the performances of SMB and Varicol processes. An equilibrium stage model was used to maximize PR and extract purity simultaneously. Wongso et al.[17,18] optimized SMB and Varicol processes for the enantioseparation of a racemate, to achieve the highest purity and PR, the highest purity or PR for both enantiomers, or the highest feed flow rate with the lowest desorbent flow rate. Kurup et al.[19] studied the two-objective optimization for the recovery of *p*-xylene from a mixture of C8 aromatics. Their study intended to maximize the *p*-xylene recovery while minimizing the desorbent consumption or to maximize recovery and purity of *p*-xylene simultaneously. Paredes and Mazzotti[20] compared SMB and column chromatography processes which were optimized for maximum PR and minimum solvent consumption. The optimized SMB process showed superior performance and more diverse solutions. In these previous studies, however, either only operating parameters were optimized or only one or two system parameters were optimized while some operating parameters were fixed. Kurup et al.[21,22] adapted NSGA-II-JG algorithm for the multiobjective optimization of ternary-mixture separation of C8 aromatics containing xylene isomers using modified SMB systems. The objective functions were to maximize product purity of two or three components.

The previous optimization studies using the adaptations of NSGA were based on simulations which needed numerical solutions of differential equations. This approach is time-consuming if many decision variables are optimized. To obtain nondominated solutions, a large number of simulations need to be performed to search a large space. No previous studies are available with the simultaneous optimization of all the 12 operating and system parameters.

In this study, the standing wave design (SWD) is incorporated with NSGA-II-JG. SWD was first developed by Ma and Wang[23] for linear isotherm systems and further developed by Mallmann et al.,[24] Xie et al,[25] and Lee et al.[26] for

Table 1. Multiobjective Optimization Studies Using GA for SMB Separations

	Models	Objective Functions	Decision Variables	Fixed Parameters	Constraints	Optimization Method	Application
Zhang et al. (2002)	Modified Langmuir isotherm, equilibrium stage	Max purity of both products or max throughput, min DR	F^{II}, F^{III}, F^{IV}, t_s, column configuration	F^{I}, R_p, L_c, N_{tot}, C_F	Purity	NSGA	Chiral separation of 1,2,3,4-tetrahydro-1-naphthol
Subramani et al. (2003)	Linear isotherm, linear driving force-dispersive	Max PR, max purity or max PR of both products	F^{I}, F^{III}, F^{IV}, t_s, L_c, column configuration	F_{feed}, R_p, N_{tot}, C_F	Purity, PR	NSGA	Purification of fructose from a mixture of glucose and fructose solution
Zhang et al. (2003)	Langmuir isotherm, equilibrium stage	Max purity, max PR	F^{I}, F^{II}, F^{III}, F^{IV}, t_s	R_p, L_c, N_{tot}, column configuration, C_F	Purity, ΔP	NSGA	Chiral separation
Wongso et al. (2004)	Modified Langmuir isotherm, equilibrium stage	Max purity, max PR or max F_{feed}, min F_{des}	F^{II}, F^{III}, F^{IV}, t_s, L_c, column configuration	F^{I}, R_p, N_{tot}, C_F	Purity	NSGA-II-JG	Chiral separation
Wongso et al. (2005)	Bi-Langmuir isotherm, linear driving force-dispersive	Max purity of both products or max PR of both products or max purity, max PR or max PR, min F_{des}	F_{des}, F_{raf}, t_s, L_c, column configuration	F^{I}, F_{feed}, R_p, N_{tot}, C_F	Purity	NSGA-II-JG	Chiral separation
Kurup et al. (2005)	Langmuir isotherm, linear driving force-dispersive	Max yield, min DR or max yield, max purity	F^{I}, F^{III}, F^{IV}, t_s, L_c, column configuration	F_{feed}, R_p, N_{tot}, C_F	Purity, yield	NSGA-II-JG	Purification of *p*-xylene from a mixture of C_8 aromatics
Paredes and Mazzotti (2007)	Linear and Langmuir isotherm, linear driving force-dispersive	Max PR, min DR	F^{I}, F^{II}, F^{III}, F^{IV}, t_s	R_p, L_c, N_{tot}, column configuration, C_F	Purity, yield, ΔP	NSGA	pDNA polishing and chiral separation
This study	Langmuir isotherm, SWD	Max PR, min DR or max PR, max yield	F^{I}, F^{II}, F^{III}, F^{IV}, t_s, R_p, L_c, N_{tot}, column configuration, C_F		Purity, yield, ΔP	NSGA-II-JG	Chiral separation

nonlinear isotherm systems. SWD can guarantee high product purity and high yield even in the systems with significant mass-transfer resistances and axial dispersion.[23,25,26] SWD involves solving only algebraic equations, instead of solving ordinary differential equations or partial differential equations as required in the previous optimization studies using process simulations. Therefore, multiobjective optimization using SWD significantly increases the computation speed. It enables us to use a personal computer for the first time to optimize simultaneously seven system parameters and five operating parameters within hours.

The factors for cost estimation are case-dependent and SMB equipment cost functions are not yet well established for low and medium pressure systems for high-purity chiral separations. For this reason, PR, desorbent requirement (DR), and yield, which are major factors in separation costs, are chosen as objective functions to obtain general trends and conclusions.

The multiobjective optimization results of this study show that large particles and short zones can be used to increase PR, but DR must increase to maintain desired purity and yield. A higher pressure limit allows the use of smaller particles to achieve a higher PR or use less desorbent at a fixed PR. The nondominated solutions show that yield needs to be sacrificed to achieve a higher PR or vice versa. In general, short zones favor high PR, but long zones favor high yield and require less desorbent. If low-affinity solute, instead of high affinity solute, is the desired product, optimization results give higher PR and less desorbent, but the nondominated solutions are less diverse.

Theory

Standing wave design

SWD was first developed by Ma and Wang[23] to determine zone velocities and port velocity systematically and efficiently for linear isotherm systems in a continuous moving bed. For a linear isotherm system without any mass transfer resistance (defined here as a linear, ideal system), wave velocity is independent of concentration and is proportional to the interstitial velocity (Eq. 1). The key idea of SWD for an ideal system is to match the port velocity with the velocities of the desorption wave of the high affinity solute in Zone I, the desorption wave of the low affinity solute in Zone II, the adsorption wave of the high affinity solute in Zone III, and the adsorption wave of the low affinity solute in Zone IV (Figure 1). As such, the individual waves remain "standing" with respect to the ports in a continuous moving bed system, or "confined" within the respective zones in an SMB system. As a result, 100% product purity and 100% yield can be achieved simultaneously for a linear, ideal system.

$$u_{w2}^{I} = \frac{u_0^{I}}{(1 + P\delta_2^{I})} = v \tag{1a}$$

$$u_{w1}^{II} = \frac{u_0^{II}}{(1 + P\delta_1^{II})} = v \tag{1b}$$

$$u_{w2}^{III} = \frac{u_0^{III}}{(1 + P\delta_2^{III})} = v \tag{1c}$$

$$u_{w1}^{IV} = \frac{u_0^{IV}}{(1 + P\delta_1^{IV})} = v \tag{1d}$$

$$\frac{F_{feed}}{\varepsilon_b S} = (u_0^{III} - u_0^{II}) = u_{0feed} \tag{1e}$$

where the subscripts 1 and 2 denote the low-affinity solute and the high-affinity solute, respectively; the superscripts I–IV denote the four zones; u_0^j is the interstitial velocity in zone j; P is the phase ratio, defined as $(1-\varepsilon_b)/\varepsilon_b$, where ε_b is the interparticle void fraction; v is the average port velocity; F_{feed} is the feed flow rate; S is the cross-sectional area of the column; u_{0feed} is defined as the feed velocity; and δ_i^j is the retention factor of solute i in zone j. For a linear isotherm system, the retention factors are independent of solute concentrations and they are related to a_i, the linear isotherm parameters for solute i, and ε_p, the intraparticle void fraction as follows:

$$\delta_1^{II} = \varepsilon_p + (1 - \varepsilon_p)a_1 = \delta_1^{IV} \tag{2a}$$

$$\delta_2^{I} = \varepsilon_p + (1 - \varepsilon_p)a_2 = \delta_2^{III} \tag{2b}$$

In 1998, Mallmann et al.[24] extended SWD for a linear ideal system to an ideal system with Langmuir (nonlinear) isotherms.

$$q_i = \frac{a_i c_i}{(1 + \Sigma b_i c_i)} \tag{3}$$

The retention factors in Eq. 1 for a nonlinear system are concentration dependent, and they have been derived for a Langmuir system as follows:

$$\delta_2^{I} = \varepsilon_p + (1 - \varepsilon_p)a_2 \tag{4a}$$

$$\delta_1^{II} = \varepsilon_p + (1 - \varepsilon_p)\left(\frac{a_1}{1 + b_2 C_{p,2}}\right) \tag{4b}$$

$$\delta_2^{III} = \varepsilon_p + (1 - \varepsilon_p)\left(\frac{a_2}{1 + b_1 C_{s,1} + b_2 c_{s,2}}\right) \tag{4c}$$

$$\delta_1^{IV} = \varepsilon_p + (1 - \varepsilon_p)\left(\frac{a_1}{1 + b_1 C_{p,1}}\right) \tag{4d}$$

where $C_{p,i}$ is the plateau concentration of solute i, and $C_{s,i}$ is the concentration of solute i at the feed port. The extra-column dead volume delays wave migration between columns and increases retention time. The delay of retention time can be accounted for by substituting δ with the apparent retention factor, δ^*.[27]

$$\delta^* = \delta + \frac{DV}{PL_c S\varepsilon_b} \tag{5}$$

where DV is the extra-column dead volume and L_c is the single column length.

Notice that for an ideal system, if a feed velocity is unspecified, there are infinite sets of operating parameters (four

zone velocities and port velocity) that can satisfy Eqs. 1a–d, since there are five operating parameters and four equations.

If mass-transfer resistances and axial dispersion are significant in a given system (defined here as a nonideal system), the concentration waves spread, causing contaminated products. To counter this wave spreading, the interstitial velocities in Zone I and Zone II should be increased so that the desorption wave velocity of the high affinity solute (Solute 2) in Zone I and the desorption wave velocity of the low affinity solute (Solute 1) in Zone II migrate faster than the average port velocity. On the other hand, the velocities in Zones III and IV should be decreased so that the adsorption wave velocity of the high affinity solute in Zone III and that of the low affinity solute in Zone IV migrate slower than the average port velocity. The differences in the wave velocities and the port velocity counter the wave spreading and allow the individual waves to be focused in the respective zones. The velocity differences that are needed to focus the waves, and to maintain certain desired product purity and yield, have been derived and verified experimentally for nonideal systems in several previous studies.[25,26,28,29]

$$\frac{u_0^{\mathrm{I}}}{(1+P\delta_2^{\mathrm{I}})} = v + \Delta_2^{\mathrm{I}} \tag{6a}$$

$$\frac{u_0^{\mathrm{II}}}{(1+P\delta_1^{\mathrm{II}})} = v + \Delta_1^{\mathrm{II}} \tag{6b}$$

$$\frac{u_0^{\mathrm{III}}}{(1+P\delta_2^{\mathrm{III}})} = v - \Delta_2^{\mathrm{III}} \tag{6c}$$

$$\frac{u_0^{\mathrm{IV}}}{(1+P\delta_1^{\mathrm{IV}})} = v - \Delta_1^{\mathrm{IV}} \tag{6d}$$

$$\Delta_i^j = \frac{\beta_i^j}{(1+P\delta_i^j)L^j}\left(E_{\mathrm{b},i}^j + \frac{Pv^2(\delta_i^j)^2}{K_{\mathrm{f},i}^j}\right) \tag{6e}$$

where Δ_i^j is the velocity correction term, which is needed to overcome wave dispersion for solute i in zone j, L^j is the length of zone j, β_i^j is the natural logarithm of the ratio of the highest concentration to the lowest concentration of standing wave solute i in zone j, $E_{\mathrm{b},i}^i$ is the axial dispersion coefficient of solute i in zone j. $K_{\mathrm{f},i}^j$ is the lumped mass-transfer coefficient of solute i in zone j, which can be related to the particle radius (R_{p}), the intraparticle diffusivity of solute i ($D_{\mathrm{p},i}$), and the film mass-transfer coefficient of solute i in zone j ($k_{\mathrm{f},i}^j$).[23]

$$\frac{1}{K_{\mathrm{f},i}^j} = \frac{R_{\mathrm{p}}^2}{15\varepsilon_{\mathrm{p}}D_{\mathrm{p},i}} + \frac{R_{\mathrm{p}}}{3k_{\mathrm{f},i}^j} \tag{7}$$

For a nonideal system without any pressure limit, there is a maximum feed velocity which can satisfy the SWD equations for a given yield requirement. The maximum feed velocity is a function of the phase ratio, the retention factors, the lumped mass-transfer coefficients, the lengths of Zones II and III, and the yield.[26]

In practice, an SMB system has a maximum pressure limit, which can also limit the feed velocity. Lee et al.[26] incorporated a pressure limit into the SWD. The maximum pressure drop in a given system depends on zone configuration and pump configuration.[28,30] A conservative estimate was made by assuming that the desorbent pump controls the flow rates from Zones I to IV. Then, the overall system pressure can be calculated by summation of the pressure drop in each zone, which was calculated from the Ergun equation.[31]

$$\Delta P = \sum_{j=1}^{\mathrm{IV}} \Delta P^j = \sum_{j=1}^{\mathrm{IV}} L^j\left[\frac{150\mu u_0^j}{4R_{\mathrm{p}}^2}\left(\frac{1-\varepsilon_{\mathrm{b}}}{\varepsilon_{\mathrm{b}}}\right)^2 + \frac{1.75\rho(u_0^j)^2(1-\varepsilon_{\mathrm{b}})}{2R_{\mathrm{p}}\varepsilon_{\mathrm{b}}}\right] \tag{8}$$

where ΔP is the pressure drop, μ is the fluid viscosity, and ρ is the fluid density. To guarantee a product yield, zone velocities and port velocity must satisfy both Eq. 6 (the mass transfer constraint) and Eq. 8 with $\Delta P \leq \Delta P_{\max}$ (the pressure constraint). The maximum feed velocity that satisfies both Eqs. 6 and 8 with $\Delta P = \Delta P_{\max}$ gives the maximum PR as well as the minimum DR (defined below) for a given set of system parameters.

PR, DR, and yield

PR and DR represent the efficiency of an SMB separation and they are important factors in determining its separation cost.[32,33] In this study, PR is defined as the kg of product produced per kg of chiral stationary phase per day. DR is defined as the volume of desorbent required per kg of the product produced.

$$\text{PR (kg product/kg CSP/day)} = \frac{F_{\mathrm{feed}}C_{\mathrm{F},i}Y_i}{\rho_{\mathrm{bed}}\mathrm{BV}} = \frac{\varepsilon_b(u_0^{\mathrm{III}} - u_0^{\mathrm{II}})C_{\mathrm{F},i}Y_i}{\rho_{\mathrm{bed}}(N^I + N^{II} + N^{III} + N^{IV})L_{\mathrm{c}}} \tag{9}$$

$$\text{DR (L solvent/kg product)} = \frac{F_{\mathrm{des}}}{F_{\mathrm{feed}}C_{\mathrm{F},i}Y_i} = \frac{(u_o^I - u_0^{IV})}{(u_0^{\mathrm{III}} - u_0^{\mathrm{II}})C_{\mathrm{F},i}Y_i} \tag{10}$$

$$F_{\mathrm{des}} = \varepsilon_{\mathrm{b}}S(u_0^{\mathrm{I}} - u_0^{\mathrm{IV}}) \tag{11}$$

where $C_{\mathrm{F},i}$ is the feed concentration of solute i, Y_i is the yield of solute i, ρ_{bed} is the packing density, BV is the bed volume, N^j is the number of columns in each zone, and F_{des} is the desorbent flow rate. Notice that PR is a product of yield and throughput, where throughput is defined as the kg of feed processed per kg of chiral stationary phase per day.

Notice that for a linear ideal system, one can derive from Eqs. 1 and 10 that DR $= 1/C_{\mathrm{F},i}Y_i$, which is lower than the DR for a nonlinear ideal system. Nonlinear effects result in a higher DR, because δ_1^{IV} (Eq. 4d), the retention factor of the low affinity solute in Zone IV, is smaller than that of a corresponding linear system. A smaller δ_1^{IV}, in turn, results in a smaller u_0^{IV} (Eq. 1d). Since DR is proportional to $(u_0^{\mathrm{I}} - u_0^{\mathrm{IV}})$, a smaller u_0^{IV} results in a higher DR. Dispersion due to mass transfer effects also results in a higher DR, as expected from

Eq. 6. The Zone I linear velocity must increase and Zone IV velocity must decrease to overcome dispersion and to maintain the product purity and yield. For these reasons, ($u_0^{\mathrm{I}} - u_0^{\mathrm{IV}}$) is larger, resulting in a higher DR for a nonideal system than for an ideal system. The larger the particle size or the shorter the zone length, the larger the velocity correction terms are (Eq. 6), and the larger the DR.

The purity (Pu) and yield (Y) of the product i and the by-product k in the outlet streams are related by:

$$\mathrm{Pu}_i = \frac{Y_i C_{\mathrm{F},i}}{Y_i C_{\mathrm{F},i} + (1 - Y_k) C_{\mathrm{F},k}} \tag{12}$$

For chiral separation, the feed concentrations of the two enantiomers are always the same in a racemic mixture ($C_{\mathrm{F},i} = C_{\mathrm{F},k}$). Then,

$$\mathrm{Pu}_i = \frac{Y_i}{Y_i + (1 - Y_k)} \tag{13}$$

If the product i and the by-product k have the same yield ($Y_i = Y_k$), the purity of the product must have the same value as the yield.

$$\mathrm{Pu}_i = Y_i \tag{14}$$

Equation 13 can be rearranged to express the by-product yield (Y_k) as a function of the product purity (Pu_i) and yield (Y_i).

$$Y_k = \frac{\mathrm{Pu}_i - (1 - \mathrm{Pu}_i) Y_i}{\mathrm{Pu}_i} \tag{15}$$

The equation above shows that at a fixed product purity Pu_i, as product yield Y_i increases, the by-product yield Y_k must decrease.

Genetic algorithm

Simple GA. GA is a search technique inspired by Darwin's theory of evolution.[34] The algorithm starts with a population of completely random chromosomes (abstract representations of candidate solutions). Then, the fitness of each population member is evaluated and the pool is sorted with those having better fitness (representing better solutions to the problem). The better the solution is, the higher the chance it has to survive. Solutions from one generation are used to generate a new population, based on the processes of selection and reproduction of solutions through crossover and mutation. The crossover operation is performed on the randomly selected parent chromosomes and creates new offspring by exchanging the parts of a pair of parent chromosomes. After crossover is performed, mutation takes place. Mutation operation randomly changes the offspring resulted from the crossover. The radical change is intended to prevent trapping all solutions in a local optimum. These processes produce the chromosomes of the next generation which are different from those of the previous generation. Generally, the average fitness will increase by this procedure for the population. This process is repeated until some termination criterion (e.g., number of generations or improvement of the best solution) is satisfied.

Nondominated Sorting Genetic Algorithm. NSGA is different from simple GA in the selection process. Before reproduction, nondominance criterion is checked among all the chromosomes in the population. In NSGA, a ranking selection method is used to emphasize good solutions and a niche method is used for the stable diversity in the population.[35]

In NSGA-II algorithm, the concept of elitism is used to give better parents a chance to be part of the next generation. Unfortunately, this results in decrease in the diversity. The concept of JGs increases the genetic diversity in the population. This mutation allows the diversity in the mating pool by applying higher exploratory capabilities. The JGs operation is performed after the normal mutation operation in NSGA-II. A fraction of strings (selected randomly) in the population is replaced with a newly (randomly) generated binary string having the same length. Only a single JG operation was performed on a selected chromosome.

The nondominated solutions are the set of solutions in which one cannot improve a certain performance criterion without sacrificing the other. For the final decision of choosing unique optimal solution, further evaluation is needed. The nondominated set is obviously useful to narrow down the available choices.

In the optimization, a mutation operator is introduced to prevent premature convergence to local optima by randomly sampling new points in the search space. The total number of mutations in any generation is proportional to the length of the chromosome in binary bits and the mutation probability per bit. If the mutation probability per bit is kept constant in the operator, longer chromosomes have larger probabilities to undergo mutations. The higher mutation probability will reduce the effectiveness of the crossover operator in converging to the final optimal solutions. In case of smaller chromosomes, if the mutation probability per bit is too low, no mutations will occur over many generations. This may result in local minima. To prevent such problems, the mutation probability per bit is chosen to be inversely proportional to the chromosome length in binary bits, Table 2. The longer the chromosome, the smaller is the mutation probability per bit. The probability value is usually between one and two tenths of a percent. This strategy keeps the total number of mutations in any given generation relatively constant and independent of the length of the chromosome.

SMB optimization using SWD and GA

The SMB optimization problem is complicated by a relatively large number of decision variables, including continu-

Table 2. NSGA Parameters Used in the Optimization

Parameter	Value
Population size	100
Number of generations	500
Length of chromosome	53 or 68* bits
Crossover probability	0.9
Mutation probability	1/(length of chromosome in binary bits)
Jumping probability	0.65

*When product yield is added to decision variables.

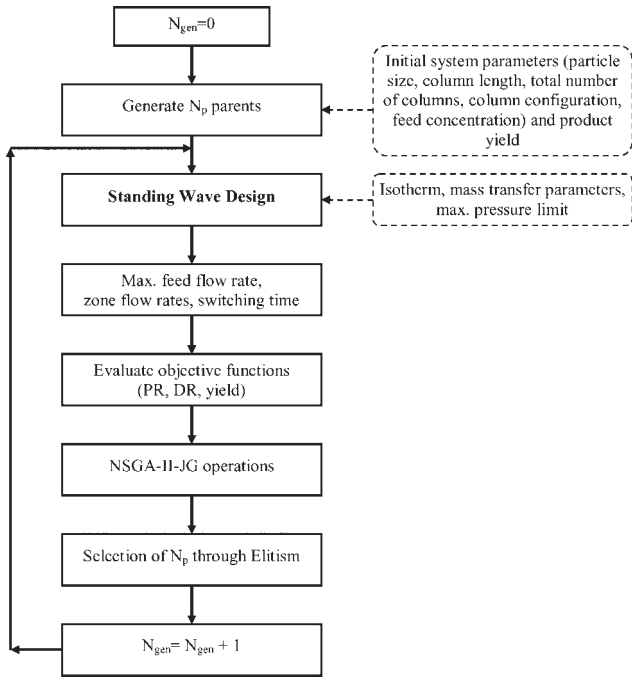

Figure 2. Schematic diagram of the NSGA optimization algorithm based on SWD.

ous variables, such as zone velocities, switching time, column length, particle size, and feed concentration, as well as discontinuous variables, such as the number of columns in each zone. GA algorithm works well for the system with both continuous and discrete variables. Although other stochastic and deterministic algorithms can also be used for the optimization of SWD, GA is chosen in this study because it is robust, does not require good initial guesses, and generates nondominated solutions efficiently.

Figure 2 shows an NSGA-II-JG optimization algorithm based on SWD. First, chromosomes that represent decision variables of system parameters (and product yield for some problems) are randomly generated and supplied to SWD algorithm. For each set of system parameters, the zone velocities and switching time that give the maximum feed velocity and simultaneously the minimum solvent consumption are determined from SWD.[26] The maximum feed velocity is limited by mass-transfer efficiency (the SWD equations, Eq. 6), or maximum pressure drop (Eq. 8), or switching time limit. Then, objective functions are calculated from the operating parameters for each set of decision variables and supplied back to NSGA-II-JG algorithm. After the selection and reproduction of chromosomes are performed in NSGA-II-JG, a new generation of population is produced. The system parameters (and product yield) in the new generation are used as the input parameters for SWD and these processes are repeated.

Table 2 lists the values of the GA parameters used in the calculation. In each optimization problem, initially 100 chromosomes were chosen and the iteration was stopped after 500 generations. Different numbers of generations (100, 200, and 500), different initial populations (100 and 200), three different random seeds (which control the initial state of the random number generator and the nature of the initial population), and three different JG operator probabilities (0.65, 0.8, and 0.9) were tested. The nondominated curves overlap with no discernible difference (within 10^{-3}) in all these cases. The seed value (0.88) used in this study gives diverse solutions. Each problem was then run with narrower bounds for 200 generations to reduce the noise in the decision variables of the solutions.

Table 3. Material Properties and Isotherm Parameters of PPA Separation System

Interparticle void fraction, ε_b	0.32
Intraparticle void fraction, ε_p	0.55
Extra-column dead volume (% of the bed volume)	5.73
D_∞ (cm^2/min)	7.47×10^{-4}
D_p (cm^2/min)	7.0×10^{-5}
k_f (cm/min)	Wilson and Geankoplis correlation
E_b (cm^2/min)	Chung and Wen correlation
Isotherms	
(+)-PPA	a = 0.448, b = 0.0102
(−)-PPA	a = 1.44, b = 0.0354

Benchmark System

Enantioseparation of norephedrine or phenylpropanolamine (PPA) was chosen as a benchmark system.[26] In the PPA separation, Chiralpak AD and methanol were used as the chiral stationary phase and the mobile phase, respectively. To test the optimization procedure based on NSGA-II-JG, we first benchmarked the single-objective optimization reported by Lee et al.[36] Table 3 shows the material properties and the isotherm parameters used in the optimization problems. Table 4 shows the bounds on the decision variables.

The bounds on switching time, column length, and particle size were chosen based on commercially available SMB equipment for a production scale of 25,000 kg/yr. The minimum switching time was set to 0.5 min. The minimum column length for large scale production is typically 10 cm, which was set to be the lower bound of column length unless noted otherwise. The upper bound of feed concentration was chosen based on the concentration range of the equilibrium isotherms for this particular example.[26] Our previous studies showed that beyond the upper bound of the feed concentration, the solution viscosity increases exponentially and can cause significant pressure drop in SMB.[26] For these two reasons, the upper bound of the feed concentration was lower than its solubility. Each zone had a lower bound of two columns because the validity of the SWD is guaranteed with two columns or more in each zone. SWD was developed based on a continuous moving bed. If an SMB system has fewer than two columns in a zone, its performance deviates

Table 4. Bounds of System Parameters

Variable	Range for Optimization
Particle diameter (μm)	5–100
Column length (cm)	10–50
Number of columns in each zone	2–5
Feed concentration (g racemate/L)	10–100
Yield*	0.8–0.9999

*For Problems 2–4.

from that of a continuous moving bed and SWD can no longer guarantee the desired product purity and yield.[23]

Compared to the grid search method used in Lee et al.,[36] single-objective optimization using NSGA-II-JG produced the same results, but at speeds of at least two orders of magnitude faster. For a typical single-objective optimization problem, the CPU time taken on an Intel Xeon™ CPU 2.4 GHz processor (using Compaq Visual Fortran) for 100 generations of NSGA-II-JG is 4 hr while that for grid search is more than 7 days.

Results and Discussion

Four two-objective optimization problems were formulated and solved to find the optimal system parameters (particle size, column length, the number of columns in each zone, and feed concentration) and operating parameters (four zone velocities and switching time). All the 12 decision variables were simultaneously optimized for these problems. In Problem 1, PR was maximized and DR was minimized while yield and purities of both the enantiomers were fixed at 0.99. In Problems 2 to 4, yield and PR are maximized. In Problem 2, yields of both the enantiomers were kept the same and maximized along with the maximization of PR. In Problems 3 and 4, yield of one of the enantiomers and PR were maximized with the purity of that enantiomer fixed at 0.99. For all the problems, three different pressure limits (1.0, 2.4, and 5.2 MPa) were considered, but the decision variables were shown only for 1.0 and 5.2 MPa. To show the effect of PR on column size, the column diameters which satisfied an annual production rate of 25,000 kg/yr with 20% downtime were calculated from the optimal feed linear velocities.

Problem 1. Maximization of PR and minimization of DR

$$\text{Max } I_1(C_{\mathrm{F},i}, L_c, N^j, R_p) = \text{PR}$$
$$\text{Min } I_2(C_{\mathrm{F},i}, L_c, N^j, R_p) = \text{DR}$$
$$\text{Subject to : } Y = 0.99 \text{ and Pu} = 0.99 \text{ for each enantiomer,}$$
$$\Delta P \le P_{\max} \textit{ and } t_s \ge 0.5 \text{ min}$$

where I_1 and I_2 are the objective functions. The bounds on the decision variables are shown in Table 4. The nondominated solutions under three different pressure limits are shown in Figure 3 when all 12 system and operating parameters are optimized simultaneously. For all pressures, at the fixed yield, a higher PR is achieved at a cost of a higher DR. Increasing the pressure limit results in increasing PR or decreasing DR. The maximum PR for a yield of 0.99 are 1.36, 1.91, 2.12 kg/kg/day for 1.0, 2.4, and 5.2 MPa, respectively. The maximum PR is limited by the purity and yield requirement, mass transfer efficiency (Eq. 6), the maximum pressure, and the bounds of the decision variables, as explained in detail later.

The minimum DR obtained is about 92.4 L/kg for all three pressures, as PR approaches to zero (Figure 3). This value is independent of the pressure limit because as the zone velocities approach to zero, the mass transfer correction terms (Eq. 6) become negligible, and the system approaches to an ideal system. This DR value can be calculated from the Zone I and Zone IV velocities for an ideal system using Eqs. 1a–e for a given feed velocity. Even though a high pressure limit can achieve lower DR at a given PR, the cost of high pressure SMB equipment is often significantly higher than that of low pressure SMB equipment. The cost function varies widely among different applications and is not considered in this study.

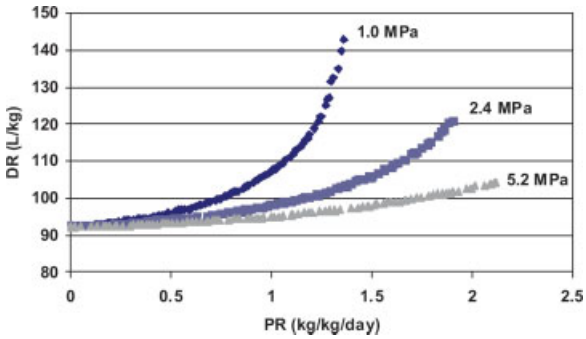

Figure 3. Comparison of nondominated optimal solutions for Problem 1 for different pressure limits.

Yield is fixed at 0.99 for both enantiomers. [Color figure can be viewed in the online issue, which is available at www.interscience.wiley.com.]

The optimal decision variables for 1.0 and 5.2 MPa are shown in Figures 4 and 5, respectively. The medium pressure results are not shown here for the sake of brevity. In all the graphs, PR is on the abscissa, and the corresponding values for the decision variable are on the ordinate. Regardless of the pressure limit, the optimal feed concentration is 100 g of racemate/L (the upper bound), and the optimal column length is 10 cm (the lower bound). As expected from Eqs. 9 and 10, high feed concentration increases PR and decreases DR. Under a given pressure limit, shorter columns or shorter zones allow higher zone velocities (Eqs. 6 and 8), which result in a higher feed velocity and higher PR (Eq. 9).

The nondominated solutions find larger particle size (Figure 4a) and smaller zone lengths (Figures 4e–h) to increase the zone velocities and the feed velocity (Figures 4c, d). As zone velocities increase, the port velocity also increases, and the corresponding switching time decreases (Figure 4b). However, to overcome wave spreading due to dispersion effects, short zones require large velocity correction terms to maintain the required product purity and yield of 0.99 (Eq. 6). The larger velocity correction terms result in higher velocity in Zone I and lower velocity in Zone IV, and therefore a larger DR. For this reason, if product purity, yield, and pressure limit are fixed, the increase in PR in the nondominated solutions is achieved at a cost of increased DR.

The highest PR (PR_{max}) at 1.0 MPa with the constraint of 0.99 yield and purity is obtained with an optimal particle size of 50.0 μm. The PR_{max} at this pressure limit can not be increased further by increasing the particle size or decreasing the zone length. The column length (10 cm) and the number of columns in each zone (2-2-2-2) have already reached to their lower bounds. Further increase in particle size will result in lower mass transfer efficiency, or smaller K_f values (Eq. 7), which will not allow solutions of Eq. 6, the standing

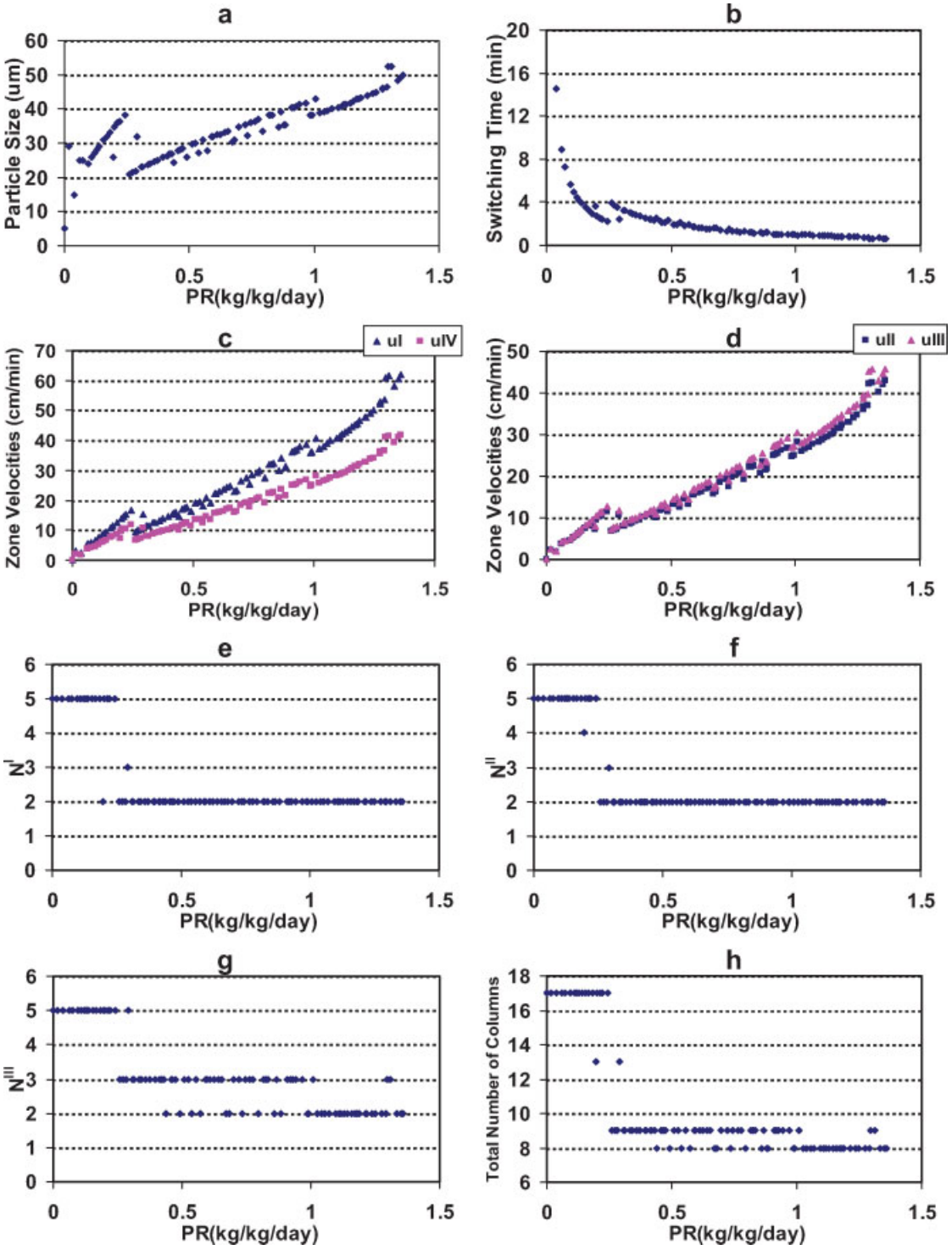

Figure 4. Nondominated solutions and corresponding decision variables for Problem 1 under 1.0 MPa pressure limit.

Yield is fixed at 0.99 for both enantiomers. The optimal feed concentration is 100 g/L, the optimal length of column is 10 cm, and the optimal number of columns in Zone IV is two for all the solutions with the PR $\geq$ 0.05 kg/kg/day. The solutions below this PR are not analyzed in detail. [Color figure can be viewed in the online issue, which is available at www.interscience.wiley.com.]

wave equations, beyond PR_{max} to maintain the yield of 0.99. In this case, the t_s at PR_{max} is 0.61 min. The PR_{max} is not limited by the minimal switching time, 0.5 min.

At a given pressure, DR can be lowered by decreasing the particle size (Figure 4a), increasing the zone lengths (Figures 4e–h), and decreasing the zone velocities (Figures 4c, d) to

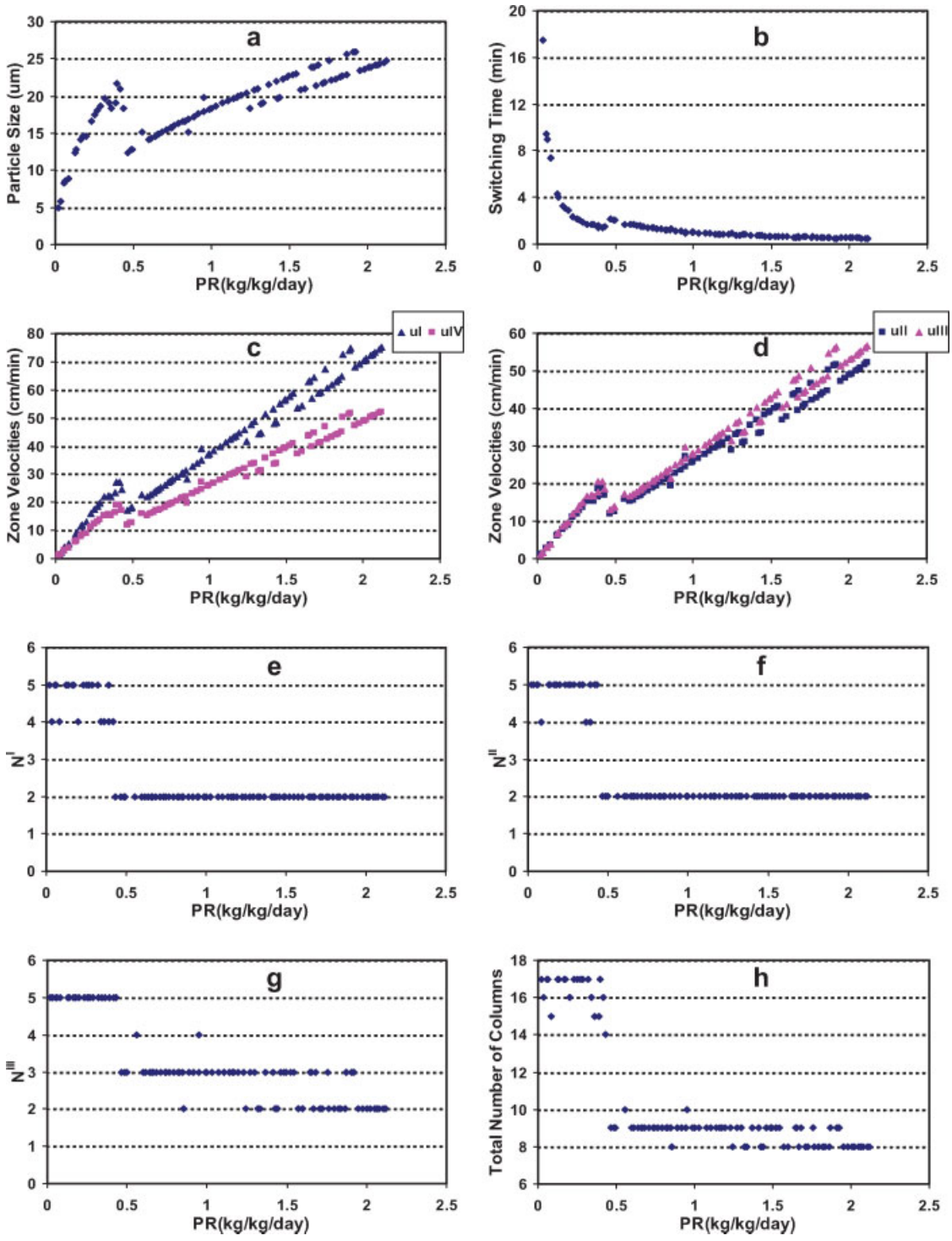

Figure 5. Nondominated solutions and corresponding decision variables for Problem 1 under 5.2 MPa pressure limit.

Yield is fixed at 0.99 for both enantiomers. The optimal feed concentration is 100 g/L, the optimal length of column is 10 cm, and the optimal number of columns in Zone IV is two for all the solutions with the PR $\geq$ 0.05 kg/kg/day. The solutions below this PR are not analyzed in detail. [Color figure can be viewed in the online issue, which is available at www.interscience.wiley.com.]

reduce the velocity correction terms (Eq. 6). However, for such systems, the feed velocities are also reduced, resulting in a very low PR.

The curves for the optimum particle size (Figure 4a) and for the optimal number of columns in each zone (Figure 4e–h) seem to be discontinuous because only integer values are

Table 5. Comparison of the Results for Maximum PR in Problem 1 When the Lower Bound of Column Length is 5 or 10 cm

Pressure limit (MPa)	1.0		2.4		5.2	
Lower bound of column length (cm)	5	10	5	10	5	10
PR_{max} (kg of product/kg of CSP/day)	2.04	1.36	2.18	1.90	2.24	2.12
DR (L/kg of product)	109.3	143.1	99.7	121.3	96.1	104.4
Particle diameter (μm)	27.5	49.8	18.1	36.5	12.4	24.7

used for the number of columns. However, different combinations of particle size and zone lengths can give the same PR and DR (within 10^{-3}). For example, for 10 cm columns, 40.4 μm particles with 2-2-2-2 configuration and 44.6 μm particles with 2-2-3-2 configuration have the same PR of 1.08 kg/kg/day. The system with the smaller particles requires a shorter Zone III to achieve the same PR at the same pressure limit. The apparent oscillations in the number of columns may be reduced further by using a more rigorous local convergence algorithm. However, the PR and DR values for the reported solutions agree to within 10^{-3}. The general trends and conclusions will not be affected by reducing the oscillations further.

The optimal decision variables for high pressure SMB (5.2 MPa) are shown in Figure 5. The general trend is similar to that of the low pressure SMB. Again, the optimal column length is 10 cm, the optimal number of columns in Zone IV is 2, and the optimal feed concentration is 100 g/L for all the nondominated solutions. The higher pressure limit allows the use of smaller particles (Figure 5a), and longer zones (Figures 5e–h) to achieve higher feed velocities and lower DR at a given PR. The smaller particles with higher mass transfer efficiency reduce the velocity correction terms, resulting in the high feed velocities and lower DR. As zone velocities increase with increasing PR, port velocity also increases, resulting in a smaller switching time (Figure 5b). In this case, the t_s at PR_{max} is 0.5 min. PR_{max} is also limited by the switching time constraint, in addition to the pressure limit and the constraints of the decision variables. Long zone lengths are also used at 5.2 MPa to reduce DR in the low PR region (Figures 5e–h).

The lower bound of column length was set at 10 cm for this problem and the optimal column length for all the nondominated solutions was found to be always 10 cm, except for the solutions of very low PR and DR. To investigate the effect of the lower bound of column length on the nondominated solutions, the lower bound was reduced from 10 to 5 cm. Table 5 shows the effect of changing the lower bound of the column length on the maximum PR. As the lower bound of the column length is reduced to 5 cm, both the optimal particle size and the optimal column length become smaller. For low pressure SMB (1.0 MPa), decreasing the column length allows the use of significantly smaller particles (Eq. 8) to achieve higher PR and lower DR. However, decreasing column length is not as beneficial for high pressure SMB (5.2 MPa). As the lower bound of column length decreases from 10 cm to 5 cm, the maximum PR for the low pressure SMB increases by 50.0% and the corresponding DR decreases by 23.6%. However, for the high pressure SMB, the maximum PR increases only by 5.7% and the corresponding DR decreases only by 8.0%. The results in Table 5 suggest that an optimal low-pressure SMB with 5-cm shallow beds with 27.5 μm particles can achieve similar PR and DR as those of an optimal high-pressure SMB system with 10 cm columns with 24.7 μm particles. The performance of low-pressure SMB can be improved significantly by a combination of shorter columns and smaller particles than those in conventional low-pressure systems.

Notice that the values of the optimal decision variables for maximal PR depend on the pressure limit and the bounds of the decision variables. We explored the nondominated solutions outside the realistic bounds of Table 2 by decreasing further the lower bound of column length to various values below 5 cm. As the lower bound decreases, the optimal column length for maximal PR is always at the lower bound of the column length, whereas the corresponding optimal particle size continues to decrease. Recall that particle size is also a decision variable, which is optimized along with all other variables. This trend continues until the lower bound of the particle size (5 μm) is reached and the corresponding "optimal" column length for 5 μm particles is 0.6 cm, which is larger than the lower bound of column length, 0.5 cm. Such "theoretically optimal" solutions, however, are difficult to implement using current technology. Shallow beds result in a very short switching time, which can not be implemented using available equipment. Uniform column packing and fluid distribution can be challenging, and the correlations for estimating axial dispersion coefficient and film mass transfer are not well established for such systems. For these reasons, only the solutions based on the realistic bounds are presented here for all the problems. Further research is needed to explore the potential of shallow beds in low pressure SMB.

If yield and pressure limit are fixed, the feed velocity and zone velocities need to be increased to increase PR. In general, PR for a given pressure limit can be increased by increasing particle size and by reducing zone lengths, which result in lower mass transfer efficiency and consequently larger DR to maintain the fixed purity and yield. Increasing the pressure limit allows the use of smaller particles to increase PR without a significant increase in DR.

Problem 2. Maximization of PR and yield (Y) of both enantiomers

$$\begin{aligned}&\text{Max } I_1(C_{\mathrm{F},i}, L_c, N^j, R_p) = \mathrm{PR}\\ &\text{Max } I_2(C_{\mathrm{F},i}, L_c, N^j, R_p) = \mathrm{Y}\\ &\text{Subject to : } \Delta P \le P_{\max},\ t_s \ge 0.5 \text{ min},\\ &\qquad\qquad \text{and } Y(-\mathrm{PPA}) = Y(+\mathrm{PPA})\end{aligned}$$

In this problem, yield is also maximized and both enantiomers are constrained to have the same yield. As a result, the purities of the two enantiomers must be the same as the

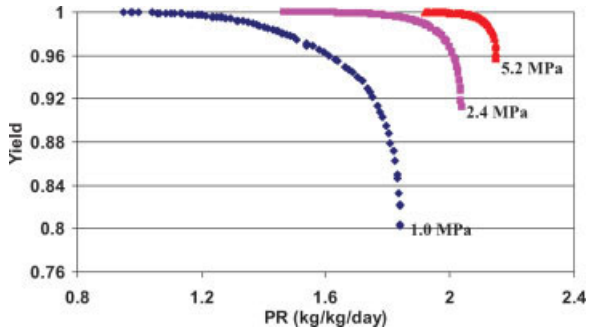

Figure 6. Comparison of nondominated solutions for Problem 2 for different pressure limits.

[Color figure can be viewed in the online issue, which is available at www.interscience.wiley.com.]

yield (Eq. 14). Figure 6 shows a trade-off between yield and PR for all the nondominated solutions at three pressures. Notice that PR is proportional to the product yield and the feed velocity and inversely proportional to the total zone length (Eq. 9). As yield increases, product purity must also increase (Eq. 14). With increasing purity and yield, β values also increase.[23] As expected from Eq. 6, the feed velocity must decrease and the zone length must increase to satisfy the high purity requirement. For this reason, a higher yield can only be obtained at a cost of a lower PR or vice versa.

The optimal decision variables for 1.0 and 5.2 MPa for Problem 2 are shown in Figures 7 and 8, respectively. Regardless of the pressure limit, the optimal column length is 10 cm (the lower bound) and the optimal feed concentration is 100 g of racemate/L (the upper bound).

The solution at 1.0 MPa for Problem 2 at a yield of 0.99 (for both enantiomers) is the same as that for Problem 1, which has a PR_{max} of 1.36. PR is increased further in Problem 2 by reducing the yield and purity of both enantiomers to below 0.99. The increase in PR is accomplished by increasing the particle size (Figure 7a), the zone and feed velocities (Figures 7c, d) until the lower bound of the switching time (or the maximal port velocity) is reached at PR = 1.7 (Figure 7b). Beyond PR = 1.7, one can not increase PR further by increasing the particle size because of the mass transfer limitation. A small increase in PR from 1.7 to 1.8 is obtained by slightly increasing the Zone III velocities and reducing the Zone II velocities (Figure 7d), whereas the zone length (Figures 7e, f) and all the other decision variables have reached their limits. In this narrow PR region, the significant decrease in DR (Figure 7g) results from a decrease in the Zone I velocity and an increase in the feed velocity.

Notice that PR can not be increased beyond a yield of 0.8 by further reducing the yield. This is because PR is defined as a product of throughput and yield (Eq. 9). Beyond a certain yield (defined here as the critical yield), although throughput can be further increased at a cost of reduced yield by optimizing the decision variables, a small increase in throughput can not compensate a significant decrease in yield. As a result PR, which is the product of throughout and yield, actually decreases beyond the critical yield. Such solutions are inferior to the nondominated solutions in Figure 7 and they are not selected by the algorithm. For this reason, nondominated solutions are not obtained beyond the critical yield for a given pressure limit.

The nondominated solutions show that DR decreases as PR is increased at a cost of reduced yield (Figure 7g). As explained in the "Theory" section, DR is related to the velocity corrections, which are proportional to β_i^j. As yield decreases, β_i^j becomes smaller, the velocity corrections are smaller, resulting in a smaller DR. SWD finds minimum DR for a given yield and system parameters. Because of this approach, even though DR is not an explicit objective function in this problem, it is minimized by SWD. The DR values below PR = 1.36 in Problem 2 are slightly higher than those obtained in Problem 1 ($Y = 0.99$), because the yield is higher than 0.99 for these solutions.

To meet an annual production rate of 25,000 kg with 20% down time, the column diameters can be calculated based on the linear velocities. Figures 7h and 8f show that as PR increases, the column diameter decreases accordingly. The column length to diameter (L/D) ratios for the maximal PR are about 0.33 and 0.35 for 1.0 and 5.2 MPa, respectively. These ratios are similar to the reported L/D values of 0.4 for some commercial SMB systems for large scale production.[8] The L/D in commercial SMB systems range from 0.4 to 40. The results of this study indicate that to maximize PR, a small L/D ratio should be used for large scale production.

At a given yield, increasing the pressure limit allows the use of smaller particles (Figures 7a and 8a) to increase PR (Figure 6) and to reduce DR (Figures 7g and 8e), see also Table 6. The optimal particle size (25 μm) at high pressure 5.2 MPa for Problem 2 is similar to the optimal particle size at PR_{max} in Problem 1 (Figure 5). To achieve the highest PR for a given yield in Problem 2, the limits of mass transfer, pressure, and switching time are reached by employing the optimal particle size, the shortest zone lengths (10 cm columns with 2-2-2-2 configuration), and the maximum port velocity (Figure 8b). Since both switching time and zone length are already at their respective lower bounds (Figure 8b), there are limited choices of particle size and zone velocities that can satisfy both the mass transfer constraints (Eq. 6) and the pressure limit (Eq. 8). For this reason, the nondominated solutions at 5.2 MPa are less diverse than at 1.0 MPa. The trends observed for DR (Figure 8e) and column diameter (Figure 8f) are similar to those in the low pressure system (Figures 7g, h), except the DR values and the column diameters are smaller because of the smaller particle size and the higher PR, respectively.

Notice that the operating parameters in this study are obtained by solving SWD equations, Eq. 6a–e. In this method, the minimum zone velocity corrections are employed to counter wave spreading due to mass transfer resistances and to achieve the desired product purity and yield. For this reason, the minimization of DR at each PR is automatically achieved by solving Eq. 6. Many other sets of operating parameters can also achieve the desired yield and purity by employing higher zone velocity corrections than those of SWD solutions. An infinite number of such operating parameters can be found. However, SWD solutions can ensure the minimum DR for a given PR. For this reason, the optimization of DR is automatically achieved. This is a key advantage of the SWD method. If the SWD equations are

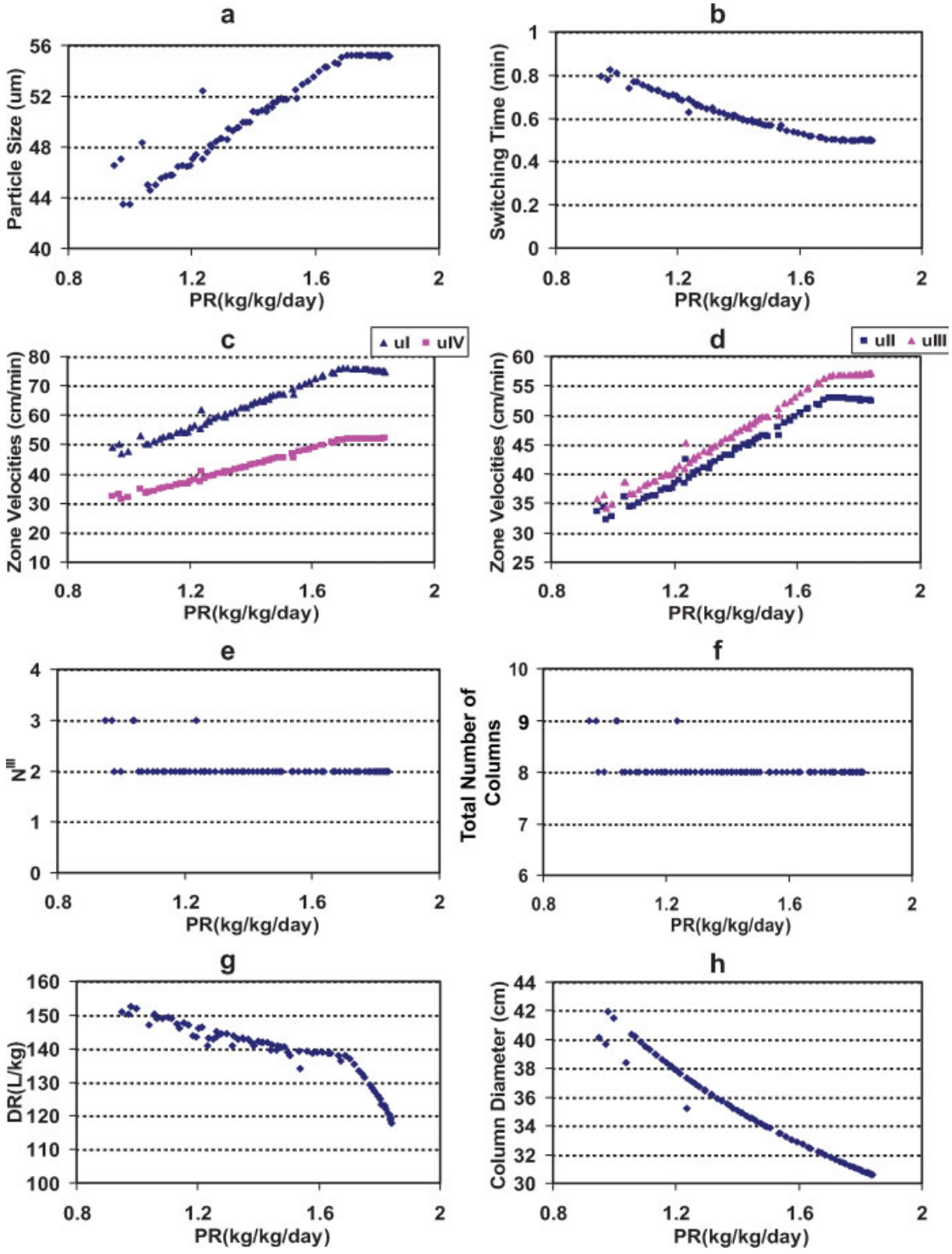

Figure 7. Nondominated solutions and corresponding decision variables for Problem 2 under 1.0 MPa pressure limit.

The optimal feed concentration is 100 g/L, the optimal length of column is 10 cm, and the optimal number of columns in Zones I, II, and IV is two for all the solutions. [Color figure can be viewed in the online issue, which is available at www.interscience.wiley.com.]

not used in the optimization algorithm and larger velocity corrections are used for finding the operating parameters, nondominated solutions can be obtained over a wider range of PR and yield. The nondominated solutions based on SWD are a subset of the general nondominated solutions and they have the minimal DR at a given PR.

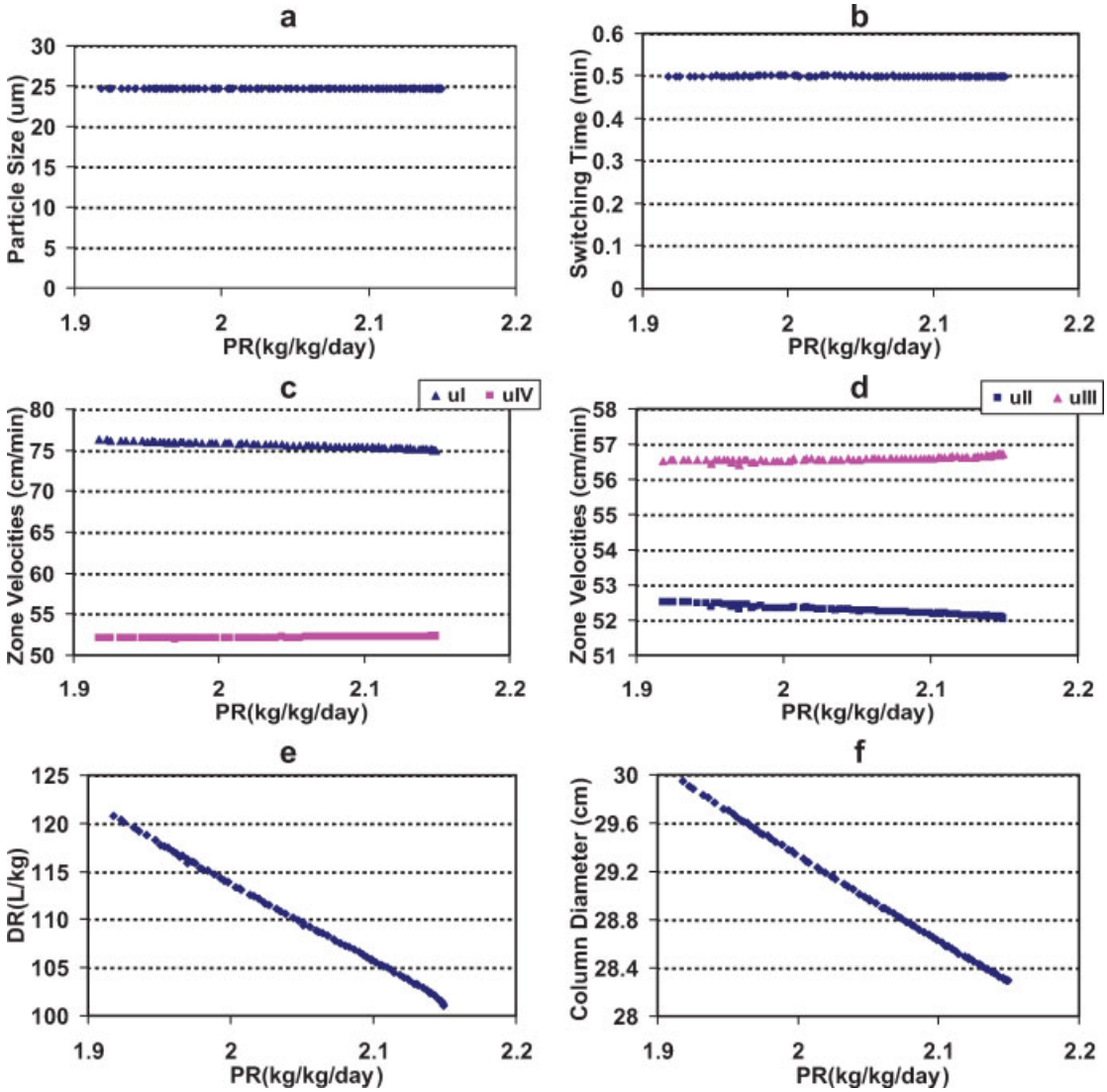

Figure 8. Nondominated solutions and corresponding decision variables for Problem 2 under 5.2 MPa pressure limit.

The optimal feed concentration is 100 g/L, the optimal length of column is 10 cm, the optimal switching time is 0.5 min, and the optimal number of columns in each Zone I–IV is two for all the solutions. [Color figure can be viewed in the online issue, which is available at www.interscience.wiley.com.]

Problem 3. Maximization of PR and Y of high affinity solute

$$\text{Max } I_1(C_{\mathrm{F},i}, L_c, N^j, R_p) = \text{PR}$$

$$\text{Max } I_2(C_{\mathrm{F},i}, L_c, N^j, R_p) = Y(-\text{PPA})$$

$$\text{Subject to : } \Delta P \le P_{\max},\ t_s \ge 0.5 \text{ min, and Pu } (-\text{PPA}) = 0.99$$

Table 6. Comparison of the Results for PR and DR at a Given Yield at High Pressure and Low Pressure in Problem 2

	5.2 MPa		1.0 MPa	
Yield	PR (kg/kg/day)	DR (L/kg)	PR (kg/kg/day)	DR (L/kg)
0.99	2.114	104.562	1.345	143.447
0.98	2.139	102.426	1.464	140.297
0.97	2.146	101.617	1.547	139.814
0.96	2.149	101.097	1.599	138.478

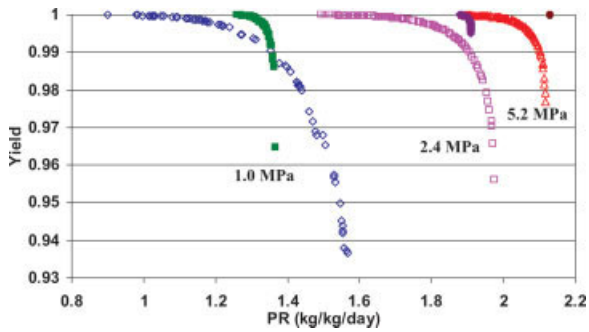

Figure 9. Comparison of nondominated solutions for Problems 3 and 4 for different pressure limits. Open: Problem 3, Closed: Problem 4.

[Color figure can be viewed in the online issue, which is available at www.interscience.wiley.com.]

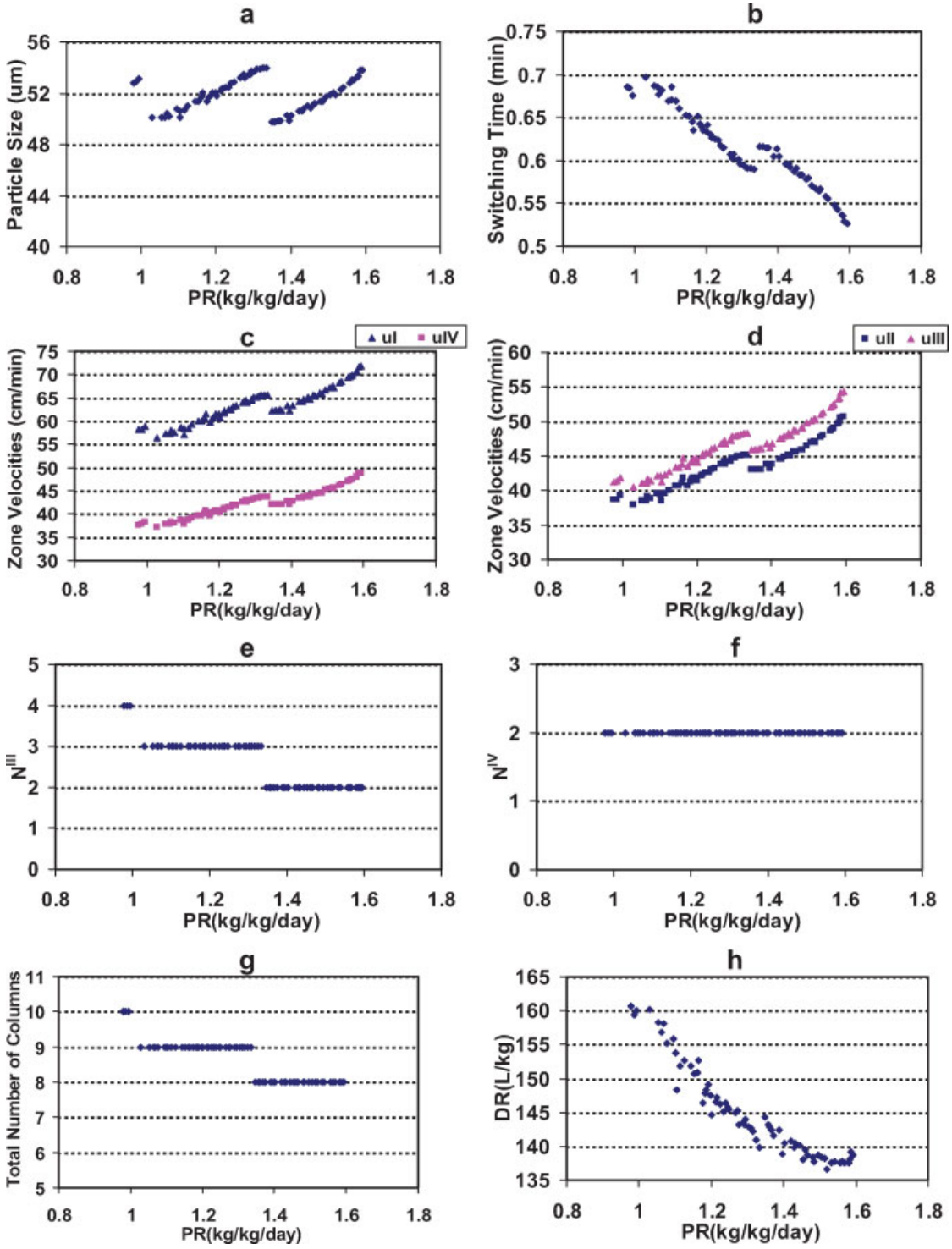

Figure 10. Nondominated solutions and corresponding decision variables for Problem 3 under 1.0 MPa pressure limit.

The optimal feed concentration is 100 g/L, the optimal length of column is 10 cm, and the optimal numbers of columns in Zones I and II are two each for all the solutions. [Color figure can be viewed in the online issue, which is available at www.interscience.wiley.com.]

In this problem, the only desired product is −PPA, which is the high-affinity solute. The purity of −PPA in the extract is fixed at 0.99. The open symbols in Figure 9 are the nondominated solutions for this problem. As PR of −PPA increases, yield decreases. As in Problem 2, increasing the pressure limit allows the use of smaller particles to increase PR and to reduce DR. The overall trend for Problem 3 (Figure 9) is similar to that of Problem 2 (Figure 6). How-

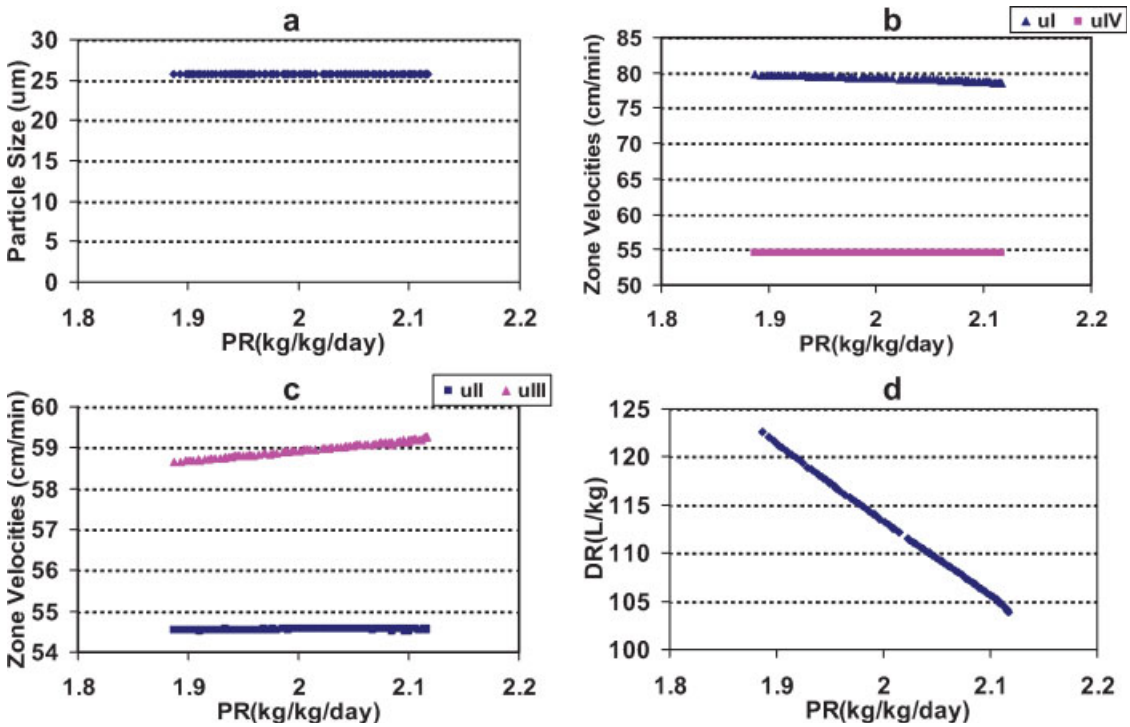

Figure 11. Nondominated solutions and corresponding decision variables for Problem 3 under 5.2 MPa pressure limit.

All the optimal solutions have a feed concentration of 100 g/L, a column length of 10 cm, a switching time of 0.5 min, and two columns in each zone. [Color figure can be viewed in the online issue, which is available at www.interscience.wiley.com.]

ever, because the purity of −PPA is fixed at 0.99 in Problem 3, the critical yield at a given pressure for this problem is higher, whereas the critical PR is lower, than for Problem 2.

The optimal decision variables are shown for 1.0 and 5.2 MPa in Figures 10 and 11, respectively. Regardless of the pressure limit, the optimal column length is 10 cm (the lower bound) and the optimal feed concentration is 100 g of racemate/L (the upper bound).

For 1.0 MPa, the optimal particle sizes are between 50 and 55 μm (Figure 10a). Around PR = 0.99 and 1.33, a decrease in the particle size (Figure 10a) and corresponding changes in t_s (Figure 10b), zone velocities (Figures 10c, d), and the number of columns in Zone III (Figures 10e–g), are used to increase PR. As in Problem 2, the PR_{max} at 1.0 MPa for Problem 3 is limited by the pressure limit and the mass transfer efficiency, but not by the minimum switching time (Figure 10b). As expected, higher velocity corrections and higher DR are required to increase yield (Figure 10h). To achieve a very high yield (>0.99), three or four columns in Zone III (the major adsorption zone for −PPA) are needed to prevent the loss of the product (Figure 10e). A long Zone III, however, increases pressure drop and limits PR. For this reason, two columns in each zone (the lower bound) are used to achieve a higher PR but at a lower yield.

For 5.2 MPa, similar trends (Figure 11) are observed for the decision variables as those for Problem 2 (Figure 8). The optimal solutions also have two columns in each zone, and the PR_{max} is also limited by the switching time. PR is increased by decreasing Zone I velocity and increasing Zone III velocity when all other decision variables reach to their limits (Figures 11b, c).

Problem 4. Maximization of PR and Y of low affinity solute

$$\text{Max } I_1(C_{F,i}, L_c, N^j, R_p) = \text{PR}$$

$$\text{Max } I_2(C_{F,i}, L_c, N^j, R_p) = Y(+\text{PPA})$$

$$\text{Subject to : } \Delta P \le P_{max},\ t_s \ge 0.5 \text{ min, and Pu } (+\text{PPA}) = 0.99$$

The low-affinity solute, +PPA, is recovered in the raffinate. In this problem, we assume that +PPA is the only desired product with a fixed purity of 0.99 and its PR and yield are maximized. In Figure 9, the closed symbols are the nondominated solutions for this problem at three pressures. The solutions again show the trade-off between yield and PR. For the same yield, higher PR and lower DR can be achieved at a higher pressure up to a critical yield. However, as the pressure limit increases, the nondominated solutions become less diverse. For 5.2 MPa, the optimal solutions converge to a very small region around PR about 2.13 kg/kg/day and yield close to 0.9999.

The optimal decision variables for 1.0 and 5.2 MPa are shown in Figures 12 and 13, respectively. Regardless of the pressure limit, the column length is 10 cm (the lower bound), the feed concentration is 100 g of racemate/L (the upper

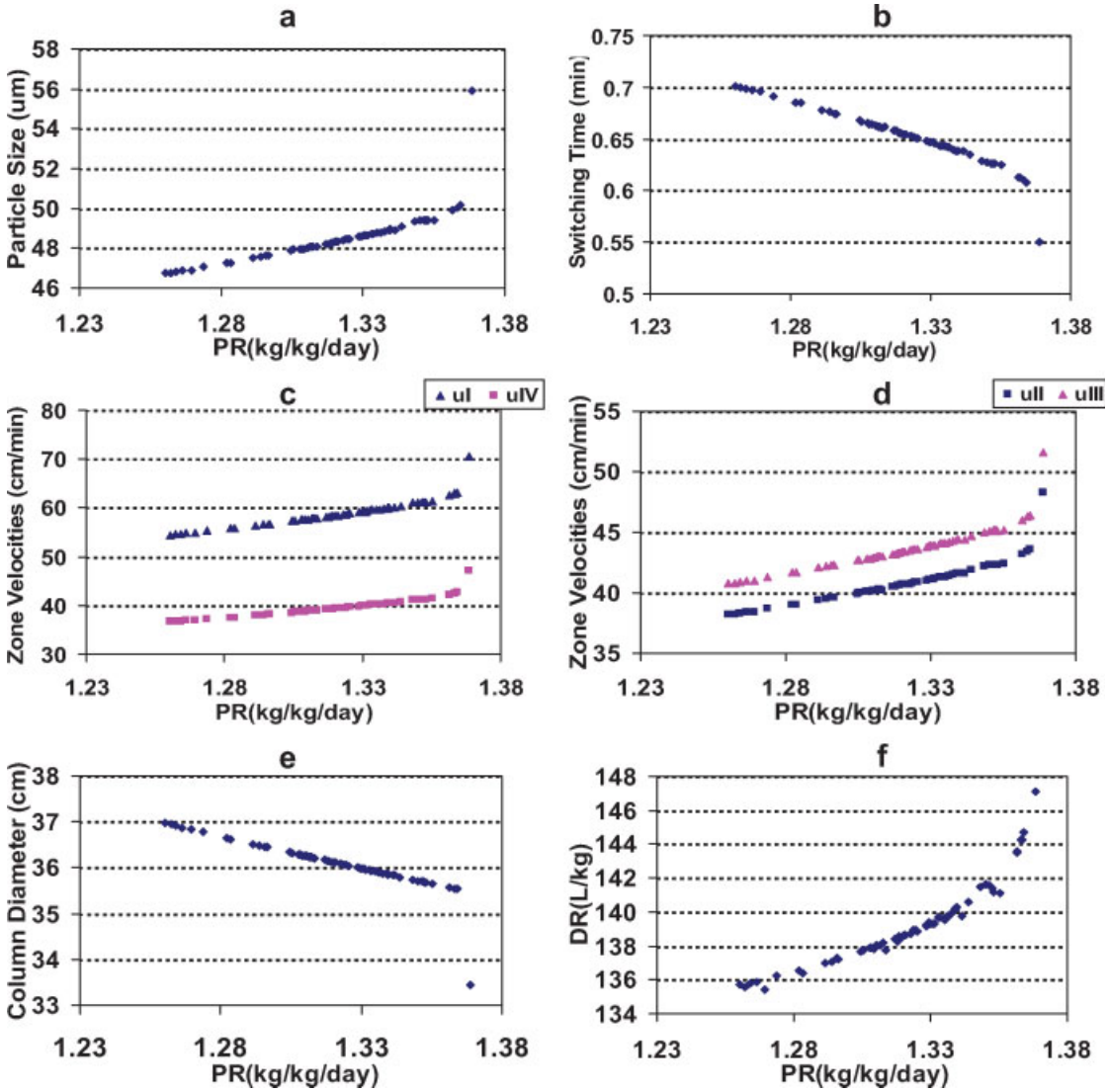

Figure 12. Nondominated solutions and corresponding decision variables for Problem 4 under 1.0 MPa pressure limit.

All the optimal solutions have a feed concentration of 100 g/L, a column length of 10 cm, and two columns in each zone. [Color figure can be viewed in the online issue, which is available at www.interscience.wiley.com.]

bound), and the total number of columns is eight with two columns in each zone (the lower bound).

For 1.0 MPa, the optimal particle size is increased to increase the zone velocities (Figures 12c, d), the feed velocity, and thus PR (Figure 12a). Because of the increased zone velocities, the port velocity increases and the switching time decreases accordingly (Figure 12b). The highest PR, however, is not limited by the minimum switching time (Figure 12b). The increase in DR with increasing PR (Figure 12f) is due to a significant decrease in the yield (Eq. 10).

For 5.2 MPa, PR is also limited by the minimum switching time, 0.5 min. At the lower bound of switching time, the optimal solutions are confined to a narrow range of PR and yield because of the high purity requirement. Since the particle size (25 μm) is constant and the zone length has also reached its lower bound, PR can be increased slightly by changing the zone velocities (Figure 13b–e). As the pressure limit increases, PR becomes larger, but the nondominated solutions become less diverse for the same reason as for Problem 2.

For the high pressure limit, the switching time and the column length reach to their lower bounds and the port velocity to its maximum (Figures 11 and 13). For the high affinity solute, its desorption wave is confined in Zone I and its adsorption wave in Zone III. To increase the yield of the high-affinity solute (Problem 3), Zone I velocity must increase, whereas Zone III velocity must decrease (Eqs. 6a, c), as shown in Figure 11. By contrast, for the low-affinity solute, its desorption wave is in Zone II and its adsorption wave is in Zone IV. To increase the yield of the low-affinity solute (Problem 4), Zone II velocity must increase, whereas Zone IV velocity must decrease (Eqs. 6b, d), as shown in Figure 13.

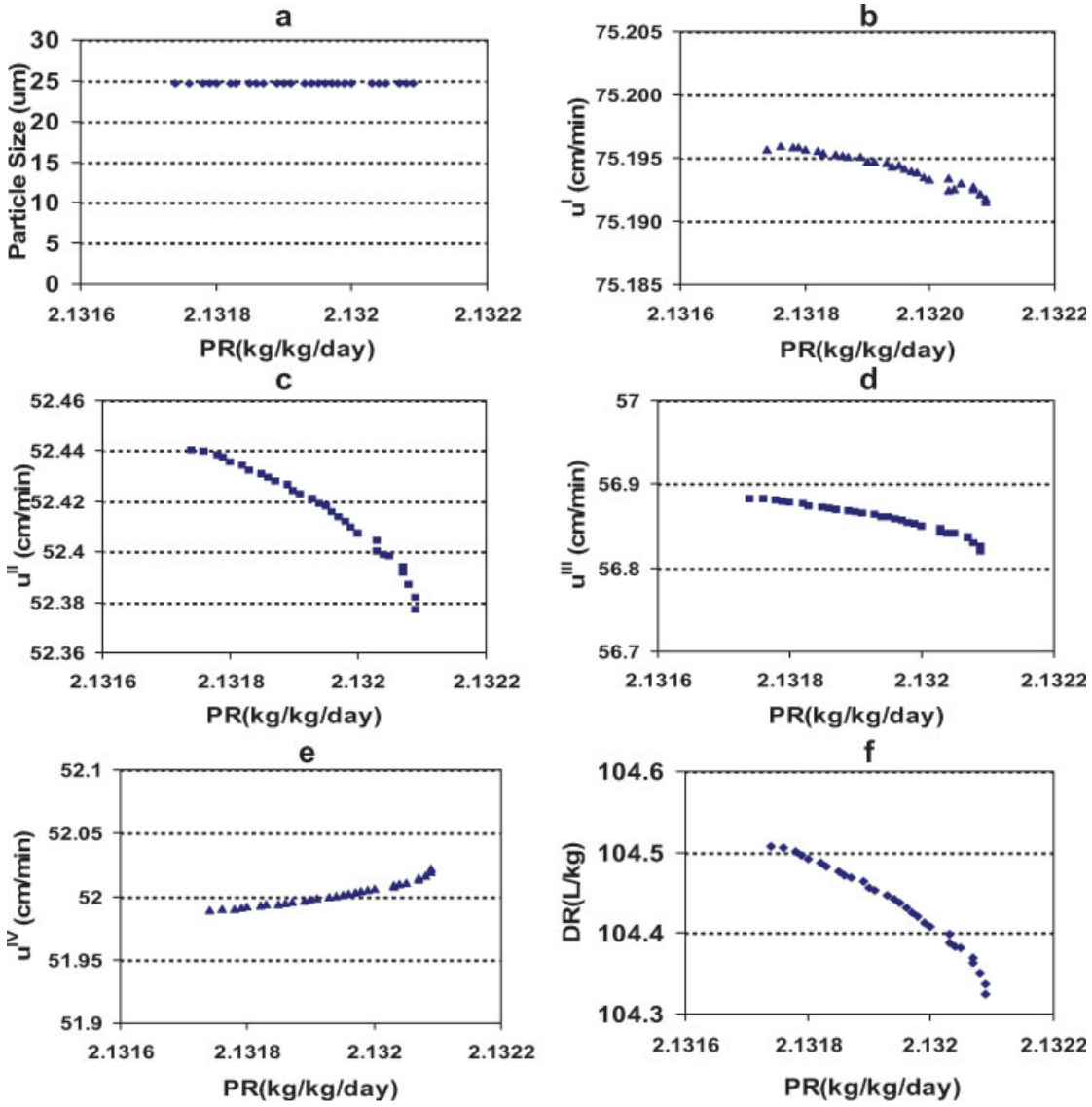

Figure 13. Nondominated solutions and corresponding decision variables for Problem 4 under 5.2 MPa pressure limit.

All the optimal solutions have a feed concentration of 100 g/L, a column length of 10 cm, a switching time of 0.5 min, and two columns in each zone. [Color figure can be viewed in the online issue, which is available at www.interscience.wiley.com.]

Compared to Problem 3, the trade-off curves of Problem 4 are narrower and provide fewer choices for the optimal solutions (Figure 9). The yield of the high-affinity solute is related to β_2^{I} and β_2^{III}, and the yield of the low-affinity solute is related to β_1^{II} and β_2^{IV}. The higher the β values, the higher the yield. For the same yield, the velocity corrections are proportional to δ^2 (Eq. 6). For this reason, to achieve the same yield in the high yield region (>0.99), the feed flow rate or PR is lower when the high-affinity solute is the product (Problem 3) than when the low-affinity solute is the product (Problem 4). The nondominated solutions of Problem 4 are less diverse because at higher PR, the constraints of pressure drop, mass-transfer efficiency, switching time, column length, and the number of columns allow fewer choices for the trade-off between yield and PR.

Conclusions

SWD was successfully incorporated with NSGA-II-JG for the optimization of SMB systems for chiral separations. The computational time is reduced by at least two orders of magnitude compared to our previous grid search method. The higher efficiency of this approach allows for the first time the simultaneous optimization of seven system parameters (particle size, column length, the numbers of columns in four zones, and feed concentration) and five operating parameters (four zone velocities and switching time). The new optimization method was used to obtain the nondominated solutions for four different multiobjective optimization problems: (1) maximization of PR and minimization of DR at a fixed yield and purity of 0.99; (2) maximization of PR and yield of both enantiomers; (3) maximization of PR and yield of the

high-affinity solute at a fixed purity of 0.99; and (4) maximization of PR and yield of the low-affinity solute at a fixed purity of 0.99.

In all the problems, since the maximization of PR is one of the objective functions, the minimum column lengths and the maximum feed concentrations are obtained for all the nondominated solutions. The optimal particle size depends on the pressure limit and the minimum column length. Increasing the pressure limit allows the use of smaller particles to increase PR and decrease DR at a fixed yield. For the system studied, to achieve high PR, at a column length of 10 cm, the optimum particle sizes are between 45 and 55 μm, and 20 and 25 μm for 1.0 and 5.2 MPa, respectively. In general, high feed concentrations and short zones favor high PR, but long zones favor high yield and low DR. The performance of low-pressure SMB can be improved significantly by using shorter columns and smaller particles than those in conventional low-pressure SMB.

In Problem 1, high purity and yield (0.99) are required for both enantiomers. High enantiomer concentrations in the feed favor high PR and low DR. The nondominated solutions show that PR can be increased at a cost of increasing DR. To achieve higher PR at a given pressure, one must reduce zone lengths and increase particle size to allow higher feed velocities and zone velocities. The optimum particle size and PR_{max} for high pressure systems are constrained by the purity requirement, the pressure limit, and the bounds of all the decision variables. For the low pressure systems, similar trend is observed, except that the minimal switching time is not an active constraint. A higher pressure limit allows the use of smaller particles to increase PR without a significant increase in DR. To reduce DR at a given pressure limit, one can sacrifice PR by using smaller particles and longer Zones of I, II, and III.

In Problem 2, both enantiomers have the same purity and yield, and both yield and PR are maximized. The nondominated solutions at different pressures show that yield can be sacrificed to achieve higher PR, but up to a critical yield. Beyond this point, yield can not be decreased further to increase PR since PR is defined as a product of throughput and yield. For a given yield and purity, higher pressure allows the use of smaller particles to achieve higher PR and lower DR. At the high pressure limit, to maximize PR, switching time, column length, and column numbers reach to their lower bounds. As a result, PR can be increased only by varying the zone velocities at a cost of yield, causing the nondominated solutions to focus on a narrower range than the low pressure systems.

In Problem 3, the purity of the high affinity product is fixed (0.99), and its yield is maximized along with the maximization of PR. The nondominated solutions are less diverse than those in Problem 2 because of the additional high purity requirement. The trend in all the decision variables are similar to that of Problem 2, except at low pressure more columns in Zone III are required to maintain high purity of the high affinity product.

In Problem 4, the purity of the low affinity product is fixed (0.99), and its yield is maximized along with the maximization of PR. The velocity corrections needed to maintain the same purity and yield are lower for the low affinity solute. For this reason, Problem 4 has a higher PR and lower DR than Problem 3 in the high yield region. As a result of high PR and high purity (0.99), the constraints of the decision variables allow fewer choices for the trade-off between PR and yield. For this reason, the nondominated solutions for Problem 4 are less diverse than those in Problem 3.

The results of this study clearly show the effects of different constraints and the trade-off between the different objective functions. A major advantage of this method is that by using SWD, minimization of DR is automatically achieved in the multiobjective optimization.

Acknowledgments

This study is supported by grants from Chiral Technologies, 21st Century Research and Technology Fund, and NSF (CTS-0625189).

Notation

a_i = Langmuir isotherm parameter of solute i based on solid volume, L/L S.V.
b_i = Langmuir isotherm parameter of solute i, L/g
BV = bed volume, cm^3
$C_{F,i}$ = feed concentration of solute i, g/L
$C_{p,i}$ = plateau concentration of solute i, g/L
$C_{s,i}$ = dilution concentration of solute i at the feed port, g/L
$D_{p,i}$ = intraparticle diffusivity of solute i, cm^2/min
DR = desorbent requirement, L of solvent/kg of product
DV = extra-column dead volume, cm^3
$E^j_{b,i}$ = axial dispersion coefficient of solute i in zone j, cm^2/min
F_{des} = desorbent flow rate, cm^3/min
F_{feed} = feed flow rate, cm^3/min
$k^j_{f,i}$ = film mass transfer coefficient of solute i in zone j, cm/min
$K^j_{f,i}$ = lumped mass transfer coefficient of solute i in zone j, min^{-1}
L_c = length of a single column, cm
L^j = length of zone j, cm
$N_c{}^j$ = number of columns in zone j
P = phase ratio, defined as $(1-\varepsilon_b)/\varepsilon_b$
PR = productivity, kg of product/kg of CSP/day
R_p = particle radius, cm
S = cross-sectional area of a column, cm^2
u^j_0 = liquid interstitial velocity in zone j, cm/min
$u^j_{w,i}$ = wave velocity of standing solute i in zone j, cm/min
Y_i = yield of solute i

Greek letters

β^j_i = decay factor of standing solute i in zone j
δ^j_i = retention factor for solute i in zone j
ΔP = pressure drop, g/cm/min^2
ε_b = interparticle void fraction
ε_p = intraparticle void fraction
ρ = fluid density, g/cm^3
ρ_{bed} = packing density, g/cm^3
μ = fluid viscosity, g/cm/min
v = average port velocity, cm/min

Literature Cited

1. Schmidt-Traub H. *Preparative Chromatography*. Weinheim, Germany: Wiley-VCH, 2005.
2. Broughton DB. Production-scale adsorptive separations of liquid mixtures by simulated moving-bed technology. *Sep Sci Technol*. 1985; 19:723–736.
3. Ganetsos G, Barker PE. *Preparative and Production Scale Chromatography*. New York, NY: Marcel Dekker, 1993.
4. Gattuso MJ. UOP Sorbex(R) simulated moving-bed (SMB) technology—a cost-effective route to optically pure products. *Chim Oggi*. 1995; 13:18–22.
5. Azevedo DCS, Rodrigues AE. Fructose-glucose separation in a SMB pilot unit: modeling, simulation, design, and operation. *AIChE J*. 2001; 47:2042–2051.

6. Juza M, Mazzotti M, Morbidelli M. Simulated moving-bed chromatography and its application to chirotechnology. *Trends Biotechnol*. 2000;18:108–118.
7. McCoy M. SMB emerges as chiral technique. *Chem Eng News*. 2000;78:17–19.
8. Schulte M, Strube J. Preparative enantioseparation by simulated moving bed chromatography. *J Chromatogr A*. 2001;906:399–416.
9. Holland JH. *Adaptation in Natural and Artificial Systems*. Ann Arbor, MI: University of Michigan Press, 1975.
10. Deb K. *Multi-Objective Optimization Using Evolutionary Algorithms*. Chichester, UK: Wiley, 2001.
11. Srinivas N, Deb K. Multiobjective function optimization using nondominated sorting genetic algorithms. *Evol Comput*. 1995;2:221–248.
12. Deb K, Pratap A, Agarwal S, Meyarivan T. A fast and elitist multiobjective genetic algorithm: NSGA-II. *IEEE Trans Evol Comput*. 2002;6:182–197.
13. Kasat RB, Gupta SK. Multi-objective optimization of an industrial fluidized-bed catalytic cracking unit (FCCU) using genetic algorithm (GA) with the jumping genes operator. *Comput Chem Eng*. 2003;27:1785–1800.
14. Zhang Z, Hidajat K, Ray AK, Morbidelli M. Multiobjective optimization of SMB and Varicol process for chiral separation. *AIChE J*. 2002;48:2800–2816.
15. Subramani HJ, Hidajat K, Ray AK. Optimization of simulated moving bed and Varicol processes for glucose-fructose separation. *Chem Eng Res Des*. 2003;81:549–567.
16. Zhang Z, Mazzotti M, Morbidelli M. Multiobjective optimization of simulated moving bed and Varicol processes using a genetic algorithm. *J Chromatogr A*. 2003;989:95–108.
17. Wongso F, Hidajat K, Ray K. Optimal operating mode for enantioseparation of SB-553261 racemate based on simulated moving bed technology. *Biotechnol Bioeng*. 2004;87:704–722.
18. Wongso F, Hidajat K, Ray K. Improved performance for continuous separation of 1,1′-bi-2-naphthol racemate based on simulated moving bed technology. *Sep Purif Technol*. 2005;46:168–191.
19. Kurup AS, Hidajat K, Ray AK. Optimal operation of an industrial-scale Parex process for the recovery of p-xylene from a mixture of C_8 aromatics. *Ind Eng Chem Res*. 2005;44:5703–5714.
20. Paredes G, Mazzotti M. Optimization of simulated moving bed and column chromatography for a plasmid DNA purification step and for a chiral separation. *J Chromatogr A*. 2007;1142:56–68.
21. Kurup AS, Hidajat K, Ray AK. Comparative study of modified simulated moving bed systems at optimal conditions for the separation of ternary mixtures of xylene isomers. *Ind Eng Chem Res*. 2006;45:6251–6265.
22. Kurup AS, Hidajat K, Ray AK. Optimal operation of a pseudo-SMB process for ternary separation under non-ideal conditions. *Sep Purif Technol*. 2006;51:387–403.
23. Ma Z, Wang NHL. Standing wave analysis of SMB chromatography: linear systems. *AIChE J*. 1997;43:2488–2508.
24. Mallmann T, Burris BD, Ma Z, Wang NHL. Standing wave design of nonlinear SMB systems for fructose purification. *AIChE J*. 1998;44:2628–2646.
25. Xie Y, Farrenburg CA, Chin CY, Mun SY, Wang NHL. Design of SMB for a nonlinear amino acid system with mass-transfer effects. *AIChE J*. 2003;49:2850–2863.
26. Lee KB, Chin CY, Xie Y, Cox GB, Wang NHL. Standing-wave design of a simulated moving bed under a pressure limit for enantioseparation of phenylpropanolamine. *Ind Eng Chem Res*. 2005;44:3249–3267.
27. Xie Y, Mun SY, Kim JH, Wang NHL. Standing wave design and experimental validation of a tandem simulated moving bed process for insulin purification. *Biotechnol Prog*. 2002;18:1332–1344.
28. Xie Y, Hritzko B, Chin CY, Wang NHL. Separation of FTC-ester enantiomers using a simulated moving bed. *Ind Eng Chem Res*. 2003;42:4055–4067.
29. Lee HJ, Xie Y, Koo YM, Wang NHL. Separation of lactic acid from acetic acid using a four-zone SMB. *Biotechnol Prog*. 2004;20:179–192.
30. Chin CY, Xie Y, Alford JS, Wang NHL. Analysis of zone and pump configurations in simulated moving bed purification of insulin. *AIChE J*. 2006;52:2447–2460.
31. Ergun S. Fluid flow through packed columns. *Chem Eng Prog*. 1952;48:89–94.
32. Wu DJ, Ma Z, Wang NHL. Optimization of throughput and desorbent in SMB chromatography for paclitaxel purification. *J Chromatogr A*. 1999;855:71–89.
33. Ahuja S. *Handbook of Bioseparations*. San Diego, CA: Academic Press, 2000.
34. Vose MD. *The Simple Genetic Algorithm: Foundations and Theory*. Cambridge, MA: MIT Press, 1999.
35. Bhaskar V, Gupta SK, Ray AK. Applications of multiobjective optimization in chemical engineering. *Rev Chem Eng*. 2000;16:1–54.
36. Lee KB, Mun SY, Cauley F, Cox GB, Wang NHL. Optimal standing-wave design of nonlinear simulated moving bed systems for enantioseparation. *Ind Eng Chem Res*. 2006;45:739–752.

Manuscript received Jun. 25, 2007, and revision received Apr. 30, 2008 and final revision received July 10, 2008.